Catalysis Letters Vol. 101, Nos. 3–4, June 2005 (© 2005)
DOI: 10.1007/s10562-005-4897-z

Dehydrogenation of ethylbenzene on alumina-pillared Fe-rich saponites

L.M. Gandía[a], A. Gil[a,*], M.A. Vicente[b], and C. Belver[b]

[a]*Departamento de Química Aplicada, Edificio Los Acebos, Universidad Pública de Navarra, Campus de Arrosadía s/n, E-31006-Pamplona, Spain*
[b]*Departamento de Química Inorgánica, Universidad de Salamanca, Plaza de la Merced s/n, E-37008-Salamanca, Spain*

Received 3 January 2005; accepted 27 January 2005

An iron-rich saponite, variety griffithite, from Griffith Park, California, USA, has been pillared with hydroxy-aluminium oligomers, giving rise to very crystalline layered solids with basal spacings of 17.4–17.7 å and specific surface areas of 233–293 m^2/g. The catalytic performance of these pillared solids, and also of the natural griffithite, all after calcination at 773 K, in the dehydrogenation of ethylbenzene was evaluated. The catalytic behaviour strongly depends on the acid properties developed in the solids by the pillaring treatment.

KEY WORDS: alumina-pillared saponite; iron-rich saponite; griffithite; pillared clay; ethylbenzene dehydrogenation.

1. Introduction

Pillared interlayered clays (PILCs) are one of the most studied families of the new microporous materials developed by molecular engineering. They are synthesized by means of a multi-step process involving the exchange of the cations that compensate the charge in natural or synthetic smectitic clays by bulky inorganic polyoxocations, and the later stabilization of the intercalated solids thus generated by calcination. The first step produces a remarkable increase in the basal spacing of the clays because of the higher size of the inorganic polyoxocations compared with that of the compensating alkaline or alkaline-earth cations, while calcination transforms the intercalated polycations into metal oxide clusters by dehydration and dehydroxylation processes. These metal oxide clusters are usually referred to as the pillars; they are inserted between the clay layers and maintain them apart for a relatively large distance, avoiding their collapse and creating a porous network of molecular range dimensions. This process can be viewed in a different way, the aggregation of the metal oxide clusters being avoided by the presence of the clay layers, generating an ultradisperse hydroxy-metallic phase of the intercalating species [1–8].

The properties of the pillared clays can be tailored by controlling the parameters involved in the synthesis, such as the starting clay, the intercalating species, the intercalation solution and procedure, as well as the drying and calcination conditions. Solids with basal spacing of 18 å, thermal stability up to 973 K and high specific surface area of about 400 m^2/g can be prepared. Aluminium-pillared clays have been largely documented, the polycation $[Al_{13}O_4(OH)_{24}(H_2O)_{12}]^{7+}$, usually known as Al_{13}, is easily obtained and well known, its intercalation on clays is standarized and easily reproducible. Montmorillonite and saponite are the clays usually pillared, other smectitic clays, such as hectorite and beidellite, are scarcely used. Pillaring with polycations of Si(IV), Ti(IV), Zr(IV), Cr(III), Fe(III) or Ga(III), has also been reported [1–8].

Styrene is an important chemical, used for the production of styrene polymers and copolymers. The feedstock for all commercial styrene manufacture is ethylbenzene. This is converted to a crude styrene that requires finishing to separate out the pure product. Direct dehydrogenation of ethylbenzene accounts for 85% of commercial styrene production. The reaction is carried out in the gas-phase with steam over a catalyst consisting primarily of iron oxide. The reaction is endothermic, and can be accomplished with the reactor operating either adiabatically or isothermally, and both methods are used in practice [9]. The use of many catalysts, which mainly consist of Fe and K oxides containing one or more promoters (Mg, Ce, Cr, Mo, V, Ca), and acid solids such as zeolites and metal phosphates, has been reported. There is a continuous search for more efficient catalysts and reaction conditions; some of the new catalysts formulations proposed also involving iron oxides [10–24].

We have recently reported the use of a saponite intercalated with hydroxy-aluminium–chromium polycations as catalyst for this reaction. It was found that unpillared saponite and alumina-pillared saponite exhibited almost exclusively dehydrogenation activity, whereas the presence of chromia induced cracking activity and reduced the selectivity to styrene [25]. In the present paper, we report

* To whom correspondence should be addressed.
E-mail: andoni@unavarra.es

1011-372X/05/0600–0229/0

on the evaluation of a saponite with a high $Fe^{2+/3+}$ content in its octahedral sheets, both unpillared and pillared with aluminium-polycations, in the gas-phase ethylbenzene dehydrogenation.

2. Experimental

2.1. Preparation of the catalysts

The particle size fraction below 2 μm of griffithite (Griffith Park deposit, California, USA, supplied by Minerals Unlimited), was used as starting material. This fraction was obtained by aqueous decantation of the original basaltic rock. Its chemical composition, expressed as metal oxides percentage, is: SiO_2: 44.02; Al_2O_3: 7.35; MgO: 12.45; Fe_2O_3: 13.38; MnO: 0.48; TiO_2: 0.28; CaO: 3.68; Na_2O: 0.70 and K_2O: 0.09, and loss by ignition 17.09%, while its cation-exchange capacity (CEC) was 86 mEq/100g.

Griffithite was intercalated with aluminium oligomeric solutions obtained by careful hydrolysis of an $AlCl_3{\cdot}6H_2O$ (Panreac, PA) solution with 1 M NaOH. The OH^-/Al^{3+} ratio and final pH were 2.2 and 4.1, respectively. Under these experimental conditions, most aluminium does polymerise to $[Al_{13}\ O_4\ (OH)_{24}\ (H_2O)_{12}]^{7+}$, but other aluminium species also exist in solution [26]. The intercalating solutions were maintained at room temperature for 24 h and added to recently prepared (24 h before) suspensions of 6.0 g of the clay in 550 cm^3 of water, and stirred for 24 h. Three Al/clay ratios were considered, namely, 2.5, 5.0 and 7.5 mmol Al per gram of clay. Then, the solids were centrifuged, washed by dialysis until being free of chloride (Ag^+ test), and dried at 333 K to give the intercalated clays. Finally, calcination at 773 K for 4 h of the intercalated solids (heating rate of 1 K/min from room temperature up to 773 K), gave the pillared clays, which are designated as PGR-number, the number indicating the intercalation Al/clay ratio used. The unpillared clay, also calcined at 773 K, is designated as GR.

2.2. Characterization techniques

Elemental analyses of the solids were carried out by plasma emission spectroscopy, using a Perkin–Elmer emission spectrometer, model Plasma II. Previously, the solids were digested under pressure, in a nitric-hydrofluoric acid mixture, in a PTFE autoclave.

X-ray powder diffraction patterns were obtained on a Siemens D-500 diffractometer at 40 kV and 30 mA with filtered Cu Kα radiation. The equipment was connected to a DACO-MP microprocessor and used Diffract-AT software.

Specific surface areas were determined from the corresponding nitrogen isotherms at 77 K, obtained from a Micromeritics ASAP 2010 analyser, after outgassing the samples at 383 K for 8 h to a residual pressure of 10^{-5} mm Hg.

The total acidity of the samples was determined by temperature programmed desorption (TPD) of ammonia. Before the adsorption of ammonia at 373 K, the samples were heated at 673 K in He flow. The TPD of ammonia was determined between 373 and 673 K at 10 K/min, by on-line gas chromatography (Shimadzu GC-14A) using a thermal conductivity detector.

Ethylbenzene dehydrogenation was carried out in a tubular (6 mm i.d.) fixed-bed Pyrex glass reactor at atmospheric pressure. The reactor feed consisted of a nitrogen stream saturated with ethylbenzene (1 vol %, Riedel-de-Haën 99%). Prior to the reaction, the catalysts were treated under nitrogen flow for 30 min at 673 K. Ethylbenzene dehydrogenation reaction was performed at 673 K and W/Q ratio of 6.67×10^{-3} $g_{cat.}$ min/cm^3. On-line analysis of the product stream was performed on a Perkin Elmer Autosystem XL gas chromatograph equipped with a Carbowax 20M column connected to a FID for hydrocarbon analyses. Selectivities were defined as the mole fraction of the reacted ethylbenzene that was converted into a given product.

3. Results and discussion

We have previously reported on the characterisation of natural griffithite, studying its acid activation [27,28], and its aluminium-pillaring [29,30]. The fraction below 2 μm was very pure, and from its chemical composition given above the following structural formula of the clay, on the basis of 22 oxygen atoms, was calculated: $[Si_{6.92}\ Al_{1.08}]\ [Mg_{2.92}\ Fe_{1.58}\ Al_{0.28}\ Mn_{0.06}\ Ti_{0.04}]\ O_{20}\ (OH)_4\ [Ca_{0.62}\ Na_{0.20}\ K_{0.04}]$. It may be noticed that all iron is expressed in the chemical composition as Fe(III), but for a specific study on the reducibility of iron and pillaring ability of the reduced solids, we submitted a new fraction of this clay to chemical analysis, including Fe(II) and Fe(III) analysis, and it was found that ca. 11% of iron was as Fe(II) [31] (more complete results on Fe(II)/Fe(III) ratios for this sample have been reported by Komadel *et al.* [32], studying several fractions with different particle size).

As deduced from the structural formula of the starting clay, Fe cations occupy about a third of the octahedral positions, and the Mg/Fe ratio is 1.85; therefore, griffithite is a high iron content saponite. Fe(III) is reducible, although not as easily as in nontronite, when treating it with inorganic reducing agents as hydrazonium sulphate and sodium dithionite [31,32]. The presence of both Fe^{2+} and Fe^{3+} in the octahedral clay sheets, together with other physicochemical properties developed by the pillaring process, make these solids very interesting as potential catalysts for the ethylbenzene dehydrogenation reaction.

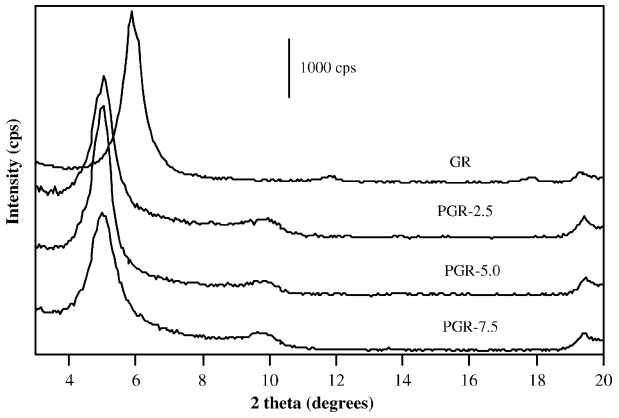

Figure 1. XRD patterns of the samples indicated.

The intercalation and pillaring processes were successfully accomplished in all cases. The X-ray diffraction patterns of the solids are shown in figure 1. The basal spacing of natural griffithite, 14.93 å, increased to about 18.8 å for the intercalated solids, which accords with the intercalation of Al_{13} polycations with their major axis perpendicular to the clay layers, the basal spacing slowly decreasing upon calcination (see table 1). The full widths at half maximum, fwhm index, adopted values of 0.53–0.65 ($2\theta°$) for the intercalated and pillared solids, indicating that they are highly ordered; the natural sample was also very crystalline (fwhm index of 0.469). Very similar results were obtained for the three Al/clay ratios considered, the fwhm indexes being always higher for the intercalated solids than for the pillared ones. It is well known that the crystallinity of the intercalated and pillared solids depends on that of the starting clay; the very high crystallinity of griffithite contributes then to the ordering of the synthesised solids.

The intercalation process gave rise to the fixation of about 9–11% Al_2O_3. The fixed amounts referred to water-free solids, and using the Si content of the natural clay as internal reference, are given in table 1 (it may be considered that no removal of SiO_2 from the clay takes place during intercalation). The amount of Al_2O_3 fixed, although similar for the several samples, slightly decreases as the Al/clay ratio increases, especially in PGR-7.5 solid. Under the assumption that all Al is fixed in the form of Al_{13} units, the numbers in table 1 are equivalent to 0.121–0.148 Al_{13} oligomers per unit cell, that is, one Al_{13} is shared by 6.8–8.3 cells. These values are relatively close to the maximum amount of Al_{13} polycations (one Al_{13} per 5.9 cells) that can be hosted in the interlayer region of smectites owing to steric constraints [33].

Other characterisation techniques, such as FT-IR spectroscopy or thermal analysis, showed for these solids the usual behaviour of intercalated and pillared solids. On the other hand, the specific surface areas of the intercalated solids (table 1) reached values very similar for the three solids and close to 300 m^2/g (35 m^2/g for natural griffithite). For PGR-2.5 and PGR-5.0 samples, a decrease in the surface area by about 20% was observed on calcining, as usually reported for this step of the preparation procedure, although in sample PGR-7.5 it remains almost constant during calcination. This suggests that, in this sample, pillars are distributed in a very homogeneous way, probably by differences in the composition of the oligomeric solutions, which may be provoked by small differences in the polymerisation conditions, induced by the higher concentration of Al in this solution. The specific surface area of the pillared solids here reported is lower than the values reported for some synthetic saponites [34], but is in accordance with the ones reported for highly pure and highly crystalline natural clays when properly pillared.

The total amount of ammonia desorbed is high for the pillared clays, with values ranging between 474 and 685 μmol/g (see table 1). In contrast, natural saponite exhibits a comparatively low total acidity, 110 μmol/g. Pyridine adsorption indicates that almost all acid sites are of Lewis type [29]. These results indicate that the formation of alumina pillars between the clay layers enhances considerably the total acidity.

To sum up, as revealed by the physicochemical characterisation, pillared griffithite catalysts are layered solids with high basal spacing of ca. 17.5 å, high surface area between 230–290 m^2/g, thermally stable and with high total acidity between 474 and 685 $\mu mol_{NH\_3}/g$, with the presence of Fe^{2+}/Fe^{3+} in the octahedral clay sheets.

The overall ethylbenzene conversion was low when using natural griffithite, about 2%, whereas values close

Table 1
Chemical analyses (main elements, water-free composition, wt%) and physicochemical properties of the samples indicated

Sample	SiO_2	Al_2O_3	Al_2O_3[a] MgO	MgO	Fe_2O_3	d(001)[b](Å)	S^c_{BET} (m^2/g)	TPD_{NH_3}($\mu mol_{NH_3}/g$)
GR*	53.21	8.88	8.88	15.05	16.17	14.93	35	110
PGR-2.5	48.36	17.96	19.76	13.69	16.13	17.42 (18.70)	255(306)	605
PGR-5.0	47.89	17.35	19.28	14.31	16.61	17.58 (18.87)	233(299)	685
PGR-7.5	49.74	16.65	17.81	13.65	16.31	17.73 (18.89)	293(294)	474

*Basal spacing and BET specific surface area correspond to the natural sample, although it was calcined at 773 K before using it as catalyst.
[a]Normalised to the SiO_2 content in natural griffithite.
[b]In parentheses, the basal spacing of the intercalated solids.
[c]In parentheses, the surface area of the intercalated solids.

to 10% after 20 min on-stream were reached over the pillared solids. The reaction products detected by gas chromatography were styrene and benzene, which resulted from ethylbenzene dehydrogenation and cracking, respectively.

The evolution with time-on-stream of the selectivities to the reaction products yielded by the various catalysts is shown in figures 2 and 3, respectively. Unpillared griffithite exhibits the highest selectivity to styrene out of all the samples considered in this study, achieving 100% selectivity to this product after 20 min on-stream at the chosen operating conditions, although this result may be significantly affected by the very low ethylbenzene conversion. In the case of the pillared solids, the selectivity to styrene continuously increases with time-on-stream; this effect being more noticeable for the griffithite sample intercalated with the highest Al/clay ratio (PGR-7.5).

The catalytic behaviour of pillared clay solids can be due to a combination of some factors. Several authors have reported that cracking and dehydrogenation activities may be related to the presence of Brönsted and Lewis acid sites [35–37]. It is well known

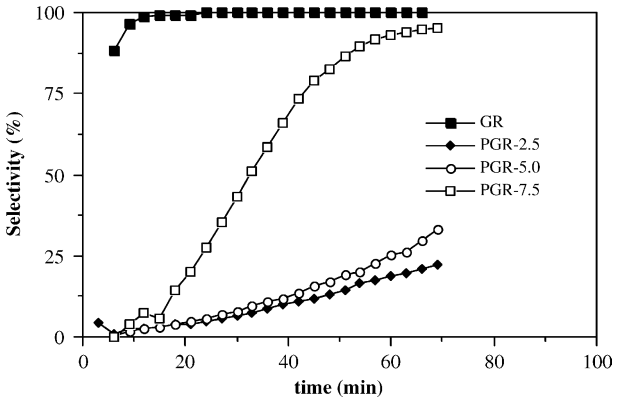

Figure 2. Evolution of the selectivity to styrene with time-on-stream for the conversion of ethylbenzene at 673 K over the catalysts indicated.

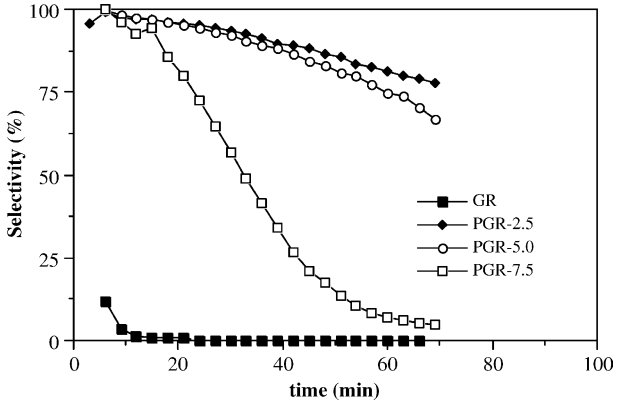

Figure 3. Evolution of the selectivity to benzene with time-on-stream for the conversion of ethylbenzene at 673 K over the catalysts indicated.

that the intercalation and pillaring of smectitic clays give rise to new acid sites, which provide the pillared solids with an additional acidity with respect to that of the starting clay [3]. Saponites have a relatively large Brönsted acidity because of their significant Al for Si isomorphous substitutions in the tetrahedral sheets. Therefore, pillaring with Al-polycations gives rise to the formation of both Brönsted and Lewis acid sites, in our solids, Lewis sites are predominant. On the other hand, the redox properties of the iron cations in the octahedral sheets may also influence strongly the catalytic behaviour of the pillared griffithite solids. All the solids presented in this work have the same Fe content, only affected by the amounts of Al fixed during pillaring. Taking into account that Fe is exclusively located in the octahedral positions of the clay layers, its accessibility is similar for the three pillared solids, and lower for the unpillared solid. Thus, the fact that the conversion achieved by the unpillared clay was noticeably lower than that achieved by the pillared solids seems in according with the characterization results.

Creation of acidity in our solids is undoubtedly related to pillaring, acidity of pillared solids is 4–6 times higher than that of natural clay. It can be established that total acidity directly depends on the number of pillars, that is, on the amount of Al fixed, and it may be proposed that the activity is governed not by the concentration of the acid sites, but for their strength and accessibility. The accessibility being very affected by the homogeneity/heterogeneity in the distribution of the pillars. Although this is rather difficult to be compared in these solids, PGR-7.5 sample seems to be, as discussed previously, the more homogeneously pillared solid in the series.

The catalytic results suggest that a relation exists between the acidity of the solids and the reaction selectivity (see table 1). Textural properties, surface area and porosity, may have a small influence in the catalytic activity of these samples. The three pillared solids have very similar basal spacing and surface area values. Besides, the chemical composition is also similar, including the Fe_2O_3 content and the amount of Al_2O_3 fixed during intercalation. For the solids with low acidity (GR and PGR-7.5), the initial significant cracking activity rapidly decreased, indicating a fast deactivation of the active sites, while simultaneously, dehydrogenation activity rapidly increased with time-on-stream. For the samples with higher acidity (PGR-2.5 and PGR-5.0), the initial cracking activity decreases slowly, with a parallel increase of the dehydrogenation activity. This trend may be only explained on the basis of the acidity of the solids. At this respect, total acidity of the solids, determined by ammonia-TPD is given in table 1, and the acidity for three temperature intervals (373–473, 473–573 and 573–673 K) is presented in figure 4. Looking at the distribution of this acidity with

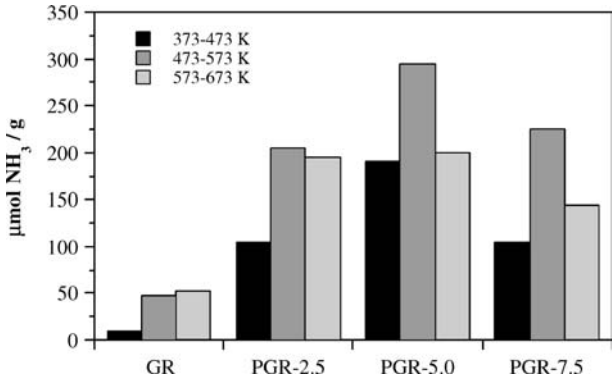

Figure 4. Acidity for various temperature intervals of the catalysts indicated.

the temperature, 'volcano'-like curves are obtained, acidity in the intermediate interval of temperature, 473–573 K, is the highest one, being even twice higher than in the 373–473 and 573–673 K intervals. Comparing with the selectivity trends observed, balancing between redox and acid sites may be considered. Unpillared griffithite has a total selectivity to styrene almost from the beginning of the reaction, the low acidity of this sample allows that the dehydrogenation reaction predominates. PGR-2.5 and PGR-5.0 samples show benzene as predominant product, selectivity to styrene increasing very slowly. PGR-7.5 show initially a high selectivity to benzene, but acid active sites are rapidly deactivated thus increasing the formation of styrene. The only unresolved question is the acidity difference between PGR-7.5 and the other two pillared catalysts, about 20–30%, difficult to be explained considering the similarity of their synthesis. Looking at the chemical composition of the solids, Al_2O_3 content seems similar for the three pillared solids. However, if the Al_2O_3 fixed during pillaring is calculated, after the subtraction of the Al_2O_3 content in the natural griffithite and normalising the amount fixed to the SiO_2 content in the griffithite, considered as an internal reference because it is expected to remain constant during pillaring, it is calculated that PGR-7.5 sample fixed 8.93% Al_2O_3, about 20% less than PGR-2.5 and PGR-5.0 samples (see table 1). This is parallel to the total concentration of acid sites in the solids, and is also in agreement with the better ordering in this solid, probably because of a better polymerisation of Al^{3+}, even if differences in the synthesis are very low.

4. Conclusions

Pillaring of a high-iron content saponite (griffithite) with hydroxy-aluminium oligomers gave rise to stable layered solids with basal spacing of 17.4–17.7 Å, and specific surface area of 233–293 m^2/g. The results of the ethylbenzene conversion at 673 K revealed that the unpillared griffithite exhibited almost exclusively dehydrogenation activity, whereas the pillaring process with hydroxy-aluminium oligomers induced cracking activity and reduced the selectivity to styrene. The overall catalytic performance was conditioned by the acidic properties of the solids, strength and nature.

Acknowledgments

The authors thank A. Meyer and E. González (Universidad del Zulia, Maracaibo, Venezuela) their help in the obtaining of the catalytic results. MAV and CB are grateful for the financial support of the Spanish Ministry of Science and Technology, MCyT, and FEDER (ref. MAT2002–03526), and from Junta de Castilla y León (ref. SA012/04). CB acknowledges a postdoctoral contract from MAT2002–03526 Grant.

References

[1] T.J. Pinnavaia, in: *Materials Chemistry, an Emerging Discipline, Advances in Chemistry Series*, L.V. Interrante, L.A. Caspar and A.B. Ellis (eds.), 245, (American Chemical Society, Washington DC, 1995) pp. 283.
[2] A. Clearfield, in: *Advances in Catalysts and Nanostructured Materials Modern Synthetic Methods*, W.R. Moser (eds.), (Academic Press, San Diego, 1996) pp. 345.
[3] J.-F. Lambert and G. Poncelet, Topics Catal. 4 (1997) 43.
[4] K. Othsuka, Chem. Mater. 9 (1997) 2039.
[5] P. Cool and E.F. Vansant, in: *Molecular Sieves-Science and Technology, Vol. 1, Synthesis*, H.G. Karge and J. Weitkamp (eds.), (Springer-Verlag, Berlin, 1998) pp. 265.
[6] J.T. Kloprogge, J. Porous Mater. 5 (1998) 5.
[7] A. Gil, L.M.ía. Gand and M.A. Vicente, Catal. Rev. – Sci. Eng. 42 (2000) 145.
[8] Z. Ding, J.T. Kloprogge, R.L. Frost, G.Q. Lu and H.Y. Zhu, J. Porous. Mater. 8 (2001) 273.
[9] D.H. James and W.M. Castor in: Ullmann's Encyclopedia of Industrial Chemistry, 7th Edition (Wiley-VCH Verlag GmbH, 2003) internet version.
[10] K. Tanabe, M. Misono, Y. Ono and H. Hattori, Stud. Surf. Sci. Catal. 51 (1989) 316.
[11] H. Miura, H. Kawai and T. Taguchi, Stud. Surf. Sci. Catal. 90 (1994) 461.
[12] F. Cavani and F. Trifirò, Appl. Catal. A 133 (1995) 219.
[13] G. Perez, A. Stefanis and A.A.G. Tomlinson, J. Mater. Chem. 7 (1997) 351.
[14] N. Mimura, I. Takahara, M. Saito, T. Hattori, K. Ohkuma and M. Ando, Catal. Today 45 (1998) 61.
[15] H.W. Weiss, D. Zscherpel and R. Schlögl, Catal. Letters 52 (1998) 215.
[16] N. Mimura and M. Saito, Catal. Today 55 (2000) 173.
[17] Y. Sakurai, T. Suzaki, N. Ikenaga and T. Suzuki, Appl. Catal. A: General 192 (2000) 281.
[18] S.T. Wong, H.P. Lin and C.Y. Mou, Appl. Catal. A: General 198 (2000) 103.
[19] A. Miyakoshi, A. Ueno and M. Ichikawa, Appl. Catal. A: General 216 (2001) 137.
[20] A. Miyakoshi, A. Ueno and M. Ichikawa, Appl. Catal. A: General 219 (2001) 249.
[21] M. Saito, H. Kimura, N. Mimura, J. Wu and K. Murata, Appl. Catal. A: General 239 (2003) 71.
[22] Y. She, J. Han and Y.H. Ma, Catal. Today 67 (2001) 43.

[23] Y. Sakurai, T. Suzaki, K. Nakagawa, N. Ikenaga, H. Aota and T. Suzuki, J. Catal. 209 (2002) 16.
[24] V.P. Vislovskiy, J.S. Chang, M.S. Park and S.E. Park, Catal. Comm. 3 (2002) 227.
[25] M.A. Vicente, A. Meyer, E. González, M.A. Bañares-Muñoz, L.M. Gandía and A. Gil, Catal. Letters 78 (2002) 99.
[26] G. Fu, L.F. Nazar and A.D. Bain, Chem. Mater. 3 (1991) 602.
[27] M.A. Vicente Rodríguez, M. Suárez Barrios, J.D. López González and M.A. Bañares-Muñoz, Clays Clay Miner. 42 (1994) 724.
[28] M.A. Vicente Rodríguez, J.D. López González and M.A. Bañares-Muñoz, Microporous Materials 4 (1995) 251.
[29] M.A. Vicente, M.A. Bañares-Muñoz, M. Suárez, J.M.M. Pozas, J.D. López González, J. Santamaría and A. Jiménez-Lopez, Langmuir 12 (1996) 5143.
[30] M.A. Vicente, M. Suárez, M.A. Bañares-Muñoz and J.M.M. Pozas, Clays Clay Miner. 45 (1997) 761.
[31] M.A. Vicente, M. Suárez, M.A. Bañares-Muñoz and J.M.M. Pozas, Clay Miner. 33 (1998) 213.
[32] P. Komadel, J. Madejová, D.A. Laird, Y. Xia and J.W. Stucki, Clay Miner. 35 (2000) 625.
[33] J.F. Lambert, S. Chevalier, R. Franck, D. Barthomeuf and H. Suquet, J.Chem. Soc. Faraday Trans. 90 (1994) 675.
[34] L. Bergaoui, J.F. Lambert, M.A. Vicente, L.J. Michot and F. Villiéras, Langmuir 11 (1995) 2849.
[35] S.M. Bradley and R.A. Kydd, J. Catal 141 (1993) 239.
[36] S. Vijayakumar, C. Vijaya, K. Rengaraj and B. Sivasankar, Bull. Chem. Soc. Jpn 67 (1994) 3107.
[37] T. Mishra and K. Parida, Appl. Catal. A: General 166 (1998) 123.